CrystEngComm

Accepted Manuscript

ROYAL SOCIETY OF CHEMISTRY

www.rsc.org/crystengcomm

Journal Name

RSCPublishing

ARTICLE

Cite this: DOI: 10.1039/x0xx00000x

Vapochromism associated with the changes in the molecular arrangement of organic crystals

Shinji Yamada,* Ayaka Katsuki, Yuka Nojiri and Yoko Tokugawa

Received ooth January 2012,
Accepted ooth January 2012

DOI: 10.1039/x0xx00000x

www.rsc.org/

Exposure of the yellow anhydrate crystals of 4'-alkoxy-4-azachalcones to water vapor gave red hydrate crystals. On the other hand, dehydration of the hydrate phase by heating recovered the anhydrate yellow phase. A comparison of the crystal structures of the anhydrate and hydrate crystals confirmed that the molecular arrangement is significantly changed during the hydration-dehydration processes: the changes in the orientation mode from head-to-tail to head-to-head, and the displacement of chloride ions and water molecules are involved in the crystal transformations. PXRD studies clarified the reversibility of the crystal transformations occurring in the hydration-dehydration processes.

Introduction

Compounds showing reversible color changes in the solid-state in response to vapor molecules have received considerable attention due to their potential utility as sensing materials.[1] Among the various vapochromic materials reported to date, MOFs[2] and metal complexes[3] have been extensively explored as they can uptake vapor molecules due to their porosity and coordination properties. On the other hand, although a number of organic crystals are known to show vapor-induced crystalline transformations,[4-7] only a few vapochromic organic crystals have been reported.[8] The origins of the vapochromism in organic crystals have been shown to conformational[5,6] and structural[7] changes in the molecules, leading to a CT interaction[5] and changes in the electronic properties.[7]

In the course of our studies on crystal engineering using cation-π interactions[9] between a pyridinium and a benzene ring,[10,11] we have reported that 4'-methoxy-4-azachalcone hydrochloride (**1a**·HCl) forms crystals with a head-to-tail columnar motif[11] stabilized by cation-π interactions. Continuing our research program, we found a new polymorphic red hydrate phase (**1a**·HCl·H_2O) that has a significantly different crystal structure from that of the yellow anhydrate phase described above. In this communication, we report the vapochromism associated with the remarkable changes in the molecular arrangement of organic crystals during in the hydration and dehydration processes (Fig. 1).

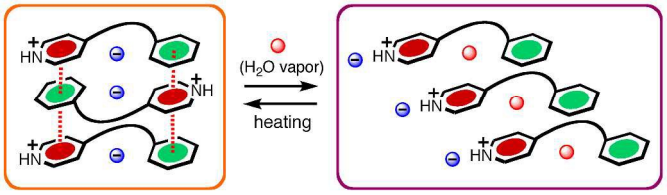

Fig. 1 Schematic representation of the crystal transformation between anhydrate and hydrate crystals with significant changes in the arrangement of molecules.

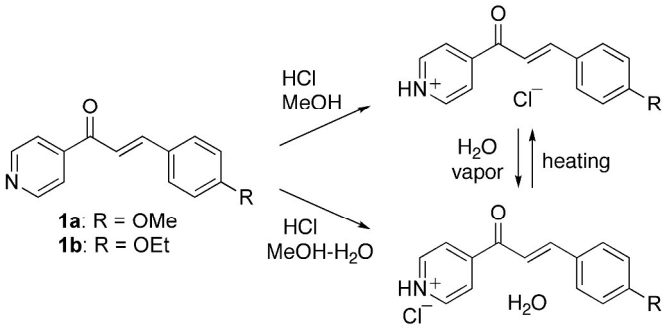

Scheme 1 Formation of hydrate and anhydrate crystals and their reversible change in a crystalline state

Experimental section

Crystallization

Crystallization of 4'-methoxy- (**1a**) and 4'-ethoxy-4-azachalcone (**1b**) from MeOH in the presence of 1.2 equiv of HCl produced yellow single crystals of **1a**·HCl and **1b**·HCl. On the other hand, crystallization from MeOH and H_2O produced red hydrate crystals **1a**·HCl·H_2O and **1b**·HCl·H_2O (Scheme 1). The yellow and red crystals are shown in Fig. 2. The hydrate

crystals contained 1.0 equiv of water molecules, which was confirmed by thermogravimetric analysis.

Crystallographic details

All measurements were made on a Rigaku R-AXIS RAPID II diffractometer using graphite monochromated Cu-Kα radiation. The data were collected at a temperature of -150 ± 1°C to a maximum 2θ value of 136.5°. The structures were solved by direct methods and expanded using SHELXS-97 program[12] and refined by full-matrix least-squares refinement on F^2 using SHELXL-97.[12] The non-hydrogen atoms were refined anisotropically. Hydrogen atoms of all CH and NH were refined using the riding model. On the other hand, hydrogen atoms of water molecules were located by the difference Fourier synthesis and refined isotropically. Figures were generated using the program Mercury.[13]

Crystal data for **1a**·HCl·H_2O: $C_{15}H_{16}O_3NCl$; red block, monoclinic, space group $P2_1/n$; a = 5.19126(15), b = 33.4280(10), c = 9.2170(3) Å; β = 112.0213(14)°; V = 1482.77(8) Å^3; Z = 4; ρ_{calcd} = 1.316 g cm^{-3}; $2\theta_{max}$ = 136.5°; T = 298(1) K; 23293 reflections collected, 2669 independent, 191 parameters; μ = 2.344 mm^{-1}; $R1$ = 0.0500 [I > 2.0σ(I)], $wR2$ = 0.1510 (all data); CCDC deposition number 1006003.

Crystal data for **1b**·HCl: $C_{16}H_{16}ClNO_2$; yellow prism, monoclinic, space group $P2_1/c$; a = 7.1274(2), b = 12.8781(3), c = 15.9623(5) Å; β = 103.450(2)°; V = 1424.95(6) Å^3; Z = 4; ρ_{calcd} = 1.351 g cm^{-3}; $2\theta_{max}$ = 136.5°; T = 123(2) K; 15692 reflections collected, 2621 independent, 182 parameters; μ = 2.379 mm^{-1}; $R1$ = 0.0371 [I > 2.0σ(I)], $wR2$ = 0.1004 (all data); CCDC deposition number 1006004.

Crystal data for **1b**·HCl·H_2O: $C_{16}H_{18}ClNO_3$; red plates, triclinic, space group P-1; a = 4.88516(18), b = 8.6653(3), c = 18.6176(7) Å; α = 86.980(3), β = 85.549(3), γ = 80.147(2)°; V = 773.52(5) Å^3; Z = 2; ρ_{calcd} = 1.321 g cm^{-3}; $2\theta_{max}$ = 136.5°; T = 123(2) K; 8223 reflections collected, 2764 independent, 198 parameters; μ = 2.344 mm^{-1}; $R1$ = 0.0549 [I > 2.0σ(I)], $wR2$ = 0.1249 (all data); CCDC deposition number 1006005.

Thermal analysis

TG/DTA measurements of the crystals of **1a**·HCl, **1b**·HCl, **1a**·HCl·H_2O and **1b**·HCl·H_2O were carried out using Bruker TG-DTA 2000SA instrument to examine the thermal stability of the crystals and to determine the wt% of the water remaining in the crystals. DSC measurements were carried out using Burker DSC3100SA. In the experiments, the samples were examined in a sealed pan under nitrogen atmosphere.

Results and Discussion

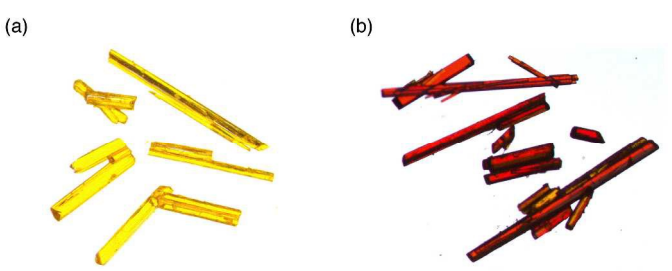

Fig. 2 Single crystals of (a) **1a**·HCl and (b) **1a**·HCl·H_2O

Crystal structures of 1a·HCl, 1a·HCl·H_2O, 1b·HCl and 1b·HCl·H_2O.

X-ray crystallographic analyses of **1a**·HCl, **1b**·HCl, **1a**·HCl·H_2O and **1b**·HCl·H_2O were then performed. The crystal structure of **1a**·HCl, which is as previously reported,[11] is shown in Fig. 3a and 3b. The molecules and chloride anions associated through the N-H···Cl$^-$ and C-H···Cl$^-$ hydrogen bonds to form a 2D sheet. The molecules were arranged in a head-to-tail manner and formed columns through cation-π interactions.

The crystal structure of **1a**·HCl·H_2O, in which 1 equiv of water molecules were involved, is shown in Fig. 3c and 3d. A comparison of the X-ray structures with those of **1a**·HCl shows that the water molecule displaced the chloride anion to form H-bonds with the substrate molecule and chloride ion via C(2)-H···O(1) and O(1)-H···Cl(2) hydrogen bonds. The chloride anion and the molecules associated through the N(1')-H···Cl(2) and C(5")-H···Cl(2) hydrogen bonds to form a 2D sheet involving a synthon with an $R_4^2(10)$ ring motif.[14] The molecules were arranged in a head-to-head and face-to-face fashion to form columns as shown in Fig. 3d. The pyridinium and benzene rings reside above and below the double bond moiety. The distances between the centroids of the double bond and those of the pyridinium and aryl moieties are 3.659 Å and 3.572 Å, respectively, suggesting that the columns are stabilized by cation-π and π-π interactions.[15] The water molecules and the chloride anions linked together through an O-H···Cl hydrogen bond to form a 1D zigzag chain motif. This chain, linked with the columns through N(1)-H···Cl(1) and C(2)-H···O(1) hydrogen bonds, assists in the formation of the head-to-head column motif. The D···A distances of O(2)-H···Cl(1), O(3)-H···Cl(1), N(1)-H···Cl(1) and C(2)-H···O(1) are 3.169(3), 3.175(3), 3.024(2) and 3.380(4) Å, respectively. The crystal structures of **1b**·HCl and **1b**·HCl·H_2O are shown in Fig. 4. Their structural features with respect to orientation modes and H-bond networks are very close to those of the crystal structures of **1a**·HCl and **1a**·HCl·H_2O, respectively.

Journal Name RSCPublishing

ARTICLE

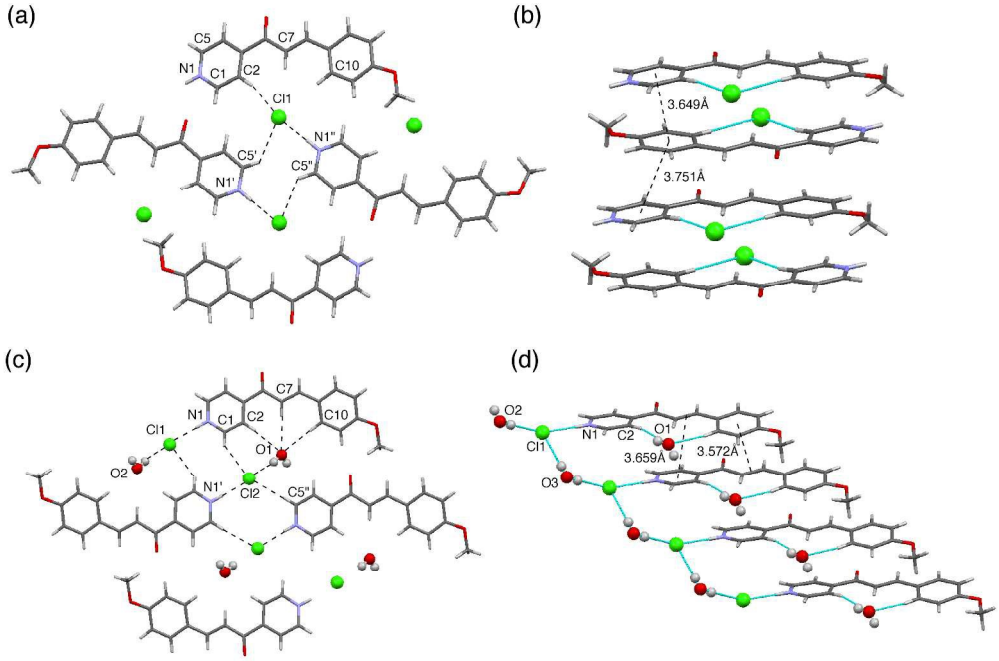

Fig. 3 Crystal structures of **1a**·HCl and **1a**·HCl·H_2O; (a) top view and (b) side view of **1a**·HCl, and (c) top view and (d) side view of **1a**·HCl·H_2O. Selected H-bond distances (Å) for **1a**·HCl: Cl1···C2 = 3.552, Cl1···C5′ = 3.500, Cl1···N1″ = 2.977. Selected H-bond distances (Å) for **1a**·HCl·H_2O: Cl1···N1 = 3.024, Cl1···O2 = 3.175, Cl1···O3 = 3.170, O1···C2 = 3.380, O1···C7 = 3.556, O1···C10 = 3.481.

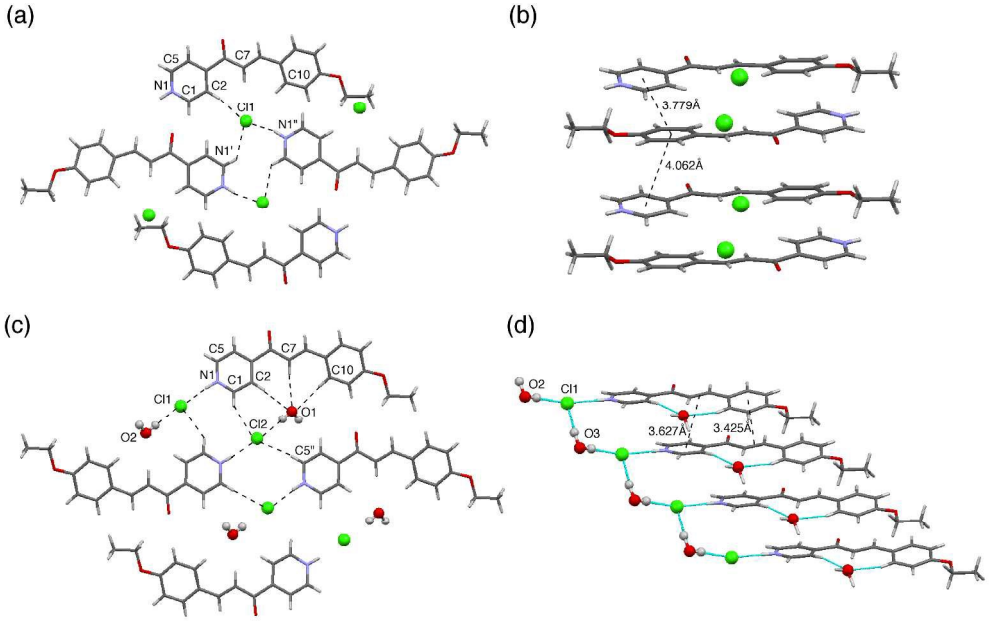

Fig. 4 Crystal structures of **1b**·HCl and **1b**·HCl·H_2O; (a) top view and (b) side view of **1b**·HCl, and (c) top view and (d) side view of **1b**·HCl·H_2O. Selected H-bond distances (Å) for **1b**·HCl: Cl1···C2 = 3.604, Cl1···C5′ = 3.471, Cl1···N1″ = 2.999. Selected H-bond distances (Å) for **1b**·HCl·H_2O: Cl1···N1 = 3.064, Cl1···O2 = 3.203, Cl1···O3 = 3.180, O1···C2 = 3.429, O1···C7 = 3.515, O1···C10 = 3.502.

Journal Name RSCPublishing

ARTICLE

Powder XRD patterns

To elucidate changes in the molecular arrangement of **1a**·HCl occurring in during the dehydration-hydration processes, we performed PXRD experiments. When the hydrate crystals of **1a**·HCl·H_2O were heated at 80°C for 5h under reduced pressure, the color of the powder turned from red to yellow. Thermogravimetric analysis of the resultant yellow powder confirmed the completion of dehydration. Fig. 5b shows the PXRD pattern of the dehydrated powder, which is in agreement with the simulation pattern of **1a**·HCl (Fig. 5a). When this anhydrous powder was kept in a desiccator with saturated water vapor for 7 days, new peaks appeared (Fig. 5c). After exposure for 10 days, the crystals turned red once more, and the PXRD pattern was in close agreement with the simulation pattern of the hydrate, showing that the anhydrous **1a**·HCl was rehydrated to produce **1a**·HCl·H_2O (Figs. 5d and 5e). Thermogravimetric analysis of the resultant red powder confirmed the completion of hydration (ESI).† These observations show the reversibility of the crystal transformation taking place during in the hydration and dehydration processes, and which involves changes from a head-to-tail to a head-to-head orientation and a displacement of the chloride anions and water molecules.

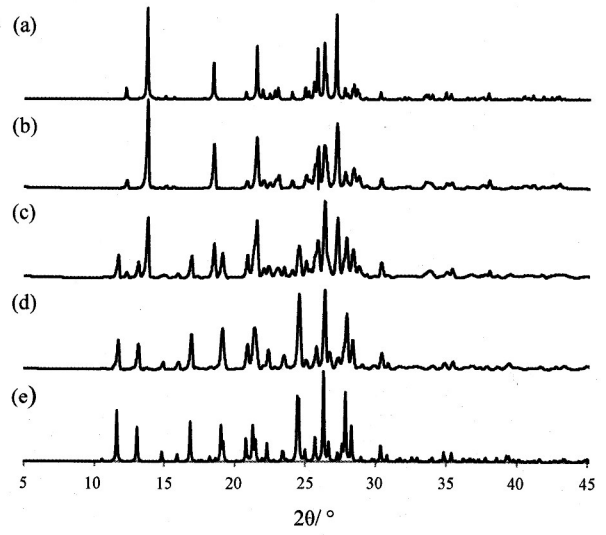

Fig. 5 Simulated PXRD patterns for (a) **1a**·HCl and (e) **1a**·HCl·H_2O, and PXRD patterns for (b) **1a**·HCl·H_2O after heating at 80°C for 5h, and the dehydrate **1a**·HCl after exposure to H_2O vapor for (c) 7 days and (d) 10 days.

Observation of crystals in open air

Although a similar phenomenon was also observed for **1b**·HCl and **1b**·HCl·H_2O, the hydration of the dehydrate **1b**·HCl was much faster than that of **1a**·HCl and give the hydrate **1b**·HCl·H_2O even in open air (ESI).† Fig. 6 clearly shows the rapid change in the color of the crystals. The red **1b**·HCl·H_2O crystals shown in Fig. 6a were dehydrated by heating at 80 °C for 5h to give yellow crystals (Fig. 6b). When these were left in open air for 5 min, the surface of the crystals turned red (Fig. 6c). After 18h, the color was restored to that before dehydration (Fig. 6d).

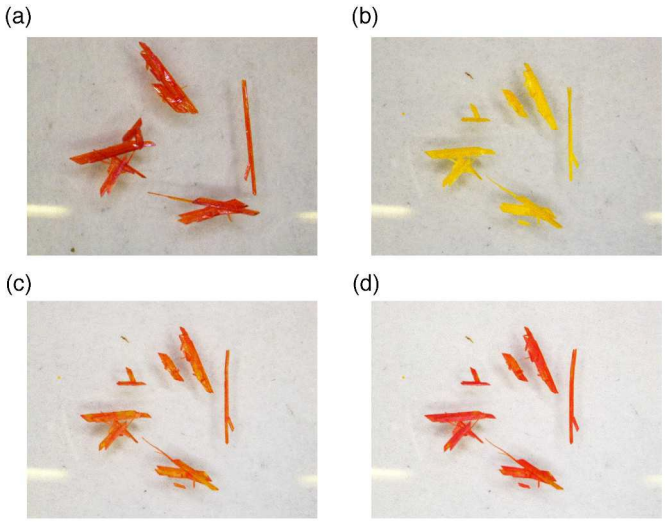

Fig.6 Single crystals of (a) **1b**·HCl·H_2O, (b) after heating at 80°C for 5h, and after being left stand for (c) 5 min and for (d) 18h in open air.

DSC experiments

Differential scanning calorimetry (DSC) measurements for the hydrate **1a**·HCl·H_2O were performed, and endotherm and exotherm peaks were observed at around 88.9 °C and 103.4 °C, respectively (Fig. 7). The endotherm corresponds to a loss of 1 equiv of water molecules, which was confirmed by thermogravimetric analysis. As the dehydrate phase upon heating was in agreement with the anhydrate phase of **1a**·HCl, as elucidated by the PXRD experiments described above, the exothermic transition could be attributed to the reorientation of the molecules from a head-to-head to a head-to-tail orientation stabilized by cation-π interactions. Similar endotherm and exotherm peaks were also observed in the DSC experiments for **1b**·HCl·H_2O.

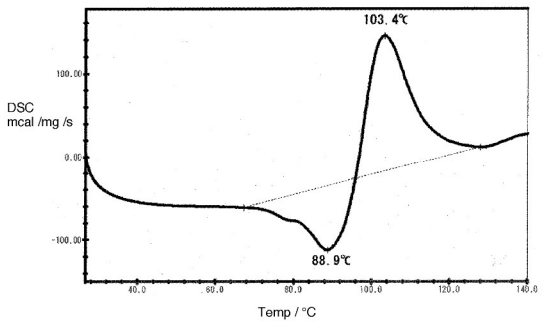

Fig. 7 DSC thermogram of **1a**·HCl·H_2O measured at a rate of 10°C/min. ΔH values for the endotherm and the exotherm were 7.8 and 16.0 kJ/mol, respectively.

UV-Vis spectra

The solid-state UV-Vis reflection spectra of the anhydrates and hydrates are shown in Fig. 8. The spectra show significant red shifts of the hydrates; the longest absorption bands for the anhydrate and hydrate of **1a** and **1b** were observed at 463 and 524 nm, and at 459 and 513 nm, respectively. The coloration of crystal is caused by intramolecular or intermolecular nature. In the present case, little conformation changes occur during the hydration-dehydration processes. The interplanar angle between two six-membered rings changed from 5.27 to 12.59 degree and from 12.43 to 15.37 degree by the hydration of **1a**·HCl and **1b**·HCl, respectively. These show that the differences in the conformations are not responsible for the color change as the increase in the interplanar angles generally causes blue shift, which is not in agreement with the observed red shift. In addition, no CT bands were observed in the absorption spectra of the hydrate crystals. Although the reason for the present remarkable red shift induced by the hydration process is still unclear, the changes in the orientation mode of the molecules and in the H-bond networks are speculated to be responsible for the red shift. Furthermore, the position of the chloride anion toward the pyridinium ring may also affect the absorption property. It has been reported that, in the opsin protein, the distance between a counter anion and an iminium moiety plays a key role in the absorption wavelength.[16] In the present system, the position of the chloride ion was also significantly changed during the hydration process.

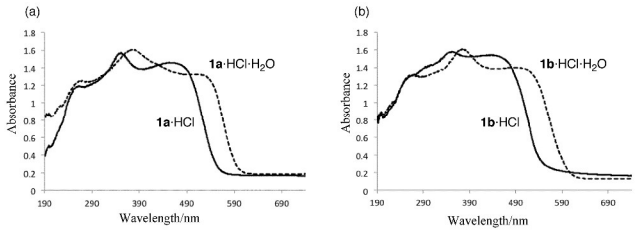

Fig. 8 Solid-state UV-Vis spectra of (a) **1a**·HCl (solid-line) and **1a**·HCl·H_2O (dashed-line), and those of (b) **1b**·HCl (solid-line) and **1b**·HCl·H_2O (dashed-line).

Conclusion

We reported the vapochromism associated with the remarkable changes in the molecular arrangement of organic crystals during the hydration-dehydration processes. To the best of our knowledge, there is no example of vapochromism involving such a remarkable changes in the crystal transformation. Although the mechanism underlying the significant red shift upon hydration is still unclear, the changes in the orientation mode and H-bond network as well as in the location of the counter ion toward the pyridinium ring are speculated to be responsible for the remarkable color change.

Notes and references

Department of chemistry, Faculty of Science, Ochanomizu University, 2-1-1 Otsuka, Bunkyo-ku, Tokyo 112-8610, Japan. E-mail: yamada.shinji@ocha.ac.jp

† Electronic Supplementary Information (ESI) available: Experimental details, TG-DTA, PXRD and crystallographic data. See DOI: 10.1039/c000000x/

1. For a review, see: S. O. Wenger, *Chem. Rev.* 2013, 113, 3686-3733.
2. For recent reports, see: (a) K. Y. Kim, S. Park, S. H. Jung, S. S. Lee, K.-M. Park, S. Shinkai and J. H. Jung, *Inorg. Chem*. 2014, **53**, 3004-3011. (b) T. K. Kim, J. H. Lee, D. Moon and H. R. Moon, *Inorg. Chem*., 2013, **52**, 589-595. (c) M.-H. Zeng, Y.-X. Tan, Y.-P. He, Z. Yin, Q. Chen and M. Kurmoo, *Inorg. Chem*. 2013, **52**, 2353-260. (d) J.-H. Wang, M. Li and D. Li, *Chem. Sci*., 2013, **4**, 1793-1801. (e) G.-B. Li, L. Li, J.-M. Liu, T. Yang and C.-Y. Su, *Cryst. Growth Des*. 2013, **13**, 1518-1525. (f) N. L. Strutt, D. Fairen-Jimenez, J. Iehl, M. B. Lalonde, R. Q. Snurr, O. K. Farha, J. T. Hupp and J. F. Stoddart, *J. Am. Chem. Soc*. 2012, **134**, 17436-17439. (g) L.Wang, S. Lu, Y. Zhou, X. Guo, Y. Lu, J. He and D. G. Evans. *Chem Comm*, 2011, **47**, 11002-11004.
3. (a) N. Kitani, N. Kuwamura, T. Tsuji, K. Tsuge and T. Konno, *Inorg. Chem*. 2014, **53**, 1949-1951. (b) A. Kobayashi, Y. Fukuzawa, H.-C. Chang and M. Kato, *Inorg. Chem*. 2012, **51**, 7508-7519. (a) X. Zhang, B. Li, Z.-H. Chen and Z.-N. Chen, *J. Mater. Chem*. 2012, **22**, 11427-11441. (b) M. Kato, *Bull. Chem. Soc. Jpn*. 2007, **80**, 287-294. (c) M. Kojima, H. Taguchi, M. Tsuchimoto and K. Nakajima, *Coord. Chem. Rev*. 2003, **237**, 183-196.
4. (a) K. Fujii, M. Aoki and H. Uekusa, *Cryst. Growth Des*. 2013, **13**, 2060-2066. (b) V. V. Chernyshev, A. V. Yatsenko, S. V. Pirogov, T. F. Nikulenkova, E. V. Tumanova, I. S. Lonin, K. A. Paseshnichenko, A. V. Mironov and Y. A. Velikodny *Cryst. Growth Des*. 2012, **12**, 6118-6125. (c) D. E. Braun, D. A. Tocher, S. L. Price and U. J. Griesser, *J. Phys. Chem. B* 2012, **116**, 3961-3972. (d) L. Seton, D. Khamar, I. Bradshaw, G. Hutcheon, *Chem. Eng. Sci.* 2012, **77**, 57-64. (e) D. Khamar, I. J. Bradshaw, G. A. Hutcheon, and L. Seton *Cryst. Growth Des*. 2012, **12**, 109-118. (f) S. Yamada and Y. Nojiri *Chem. Commun*. 2011, **47**, 9143-9145. (g) K. Fujii, H. Uekusa, N. Itoda, G. Hasegawa, E. Yonemochi, K. Terada, Z. Pan and K. D. M. Harris, *J. Phs. Chem. C* 2010, **114**, 580-586. (h) K. Fujii, Y. Ashida, H. Uekusa, F. Guo and K. D. M. Harris, *Chem Commun*., 2010, **46**, 4264-4266. (i) K. Fujii, Y. Ashida, H. Uekusa, S. Hirano, S. Toyota, F. Toda, Z. Pan and K. D. M. Harris, *Cryst. Growth Des*. 2009, **9**, 1201-1207.
5. E. Takahashi, H. Takaya and N. Takeshi, *Chem. Eur. J.* 2010, **16**, 4793-4802.

6. M. Taneda, H. Koyama and T. Kawato, *Chem. Lett.* 2007, **36**, 354-355.
7. K. Fujii, A. Sakon, A. Sekine and H. Uekusa, *Cryst. Growth Des*. 2011, **11**, 4305-4308.
8. In this paper, the examples of vapoluminescence were excluded.
9. J. C. Ma and D. A. Dougherty, *Chem. Rev.* 1997, **97**, 1303-1324.
10. (a) S. Yamada and C. Morita, *J. Am. Chem. Soc.*, 2002, **124**, 8184-8185. (b) S. Yamada, Y. Morimoto and T. Misono, *Tetrahedron Lett.* 2005, **46**, 5673-5676. (c) S. Yamada and Y. Morimoto, *Tetrahedron Lett*. 2006, **47**, 5557-5560.
11. (a) S. Yamada and Y. Tokugawa, *J. Am. Chem. Soc*. 2009, **131**, 2098-2099. (b) S. Yamada, Y. Tokugawa, Y. Nojiri and E. Takamori, *Chem. Commun*. 2012, **48**, 1763-1765.
12. G. M. Sheldrick, *Acta Crystallogr., Sect. A*, 2008, **64**, 112.
13. I. J. Bruno, J. C. Cole, P. R. Edgington, M. Kessler, C. F. Macrae, P. McCabe, J. Pearson and R. Taylor, *Acta Crystallogr.*, *Sect. B: Struct. Sci.*, 2002, **58**, 389.
14. J. Bernstein, R. E. Davis, L. Shimoni and N.-L. Chang, *Angew. Chem. Int. Ed*. 1995, **34**, 1555-1573.
15. S. Yamada, N. Sako, M. Okuda and A. Hozumi, *CrystEngComm*, 2013, **15**, 199-205.
16. M. B. Nielsen, *Chem. Soc. Rev.* 2009, **38**, 913-924.

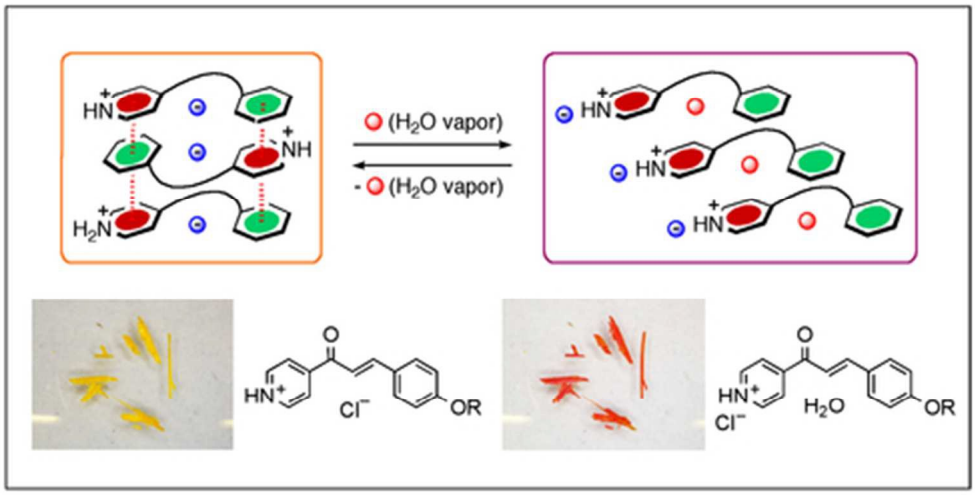

41x21mm (300 x 300 DPI)

Textual abstract for contents page

Exposure of yellow anhydrate organic crystals to water vapor gave red hydrate crystals with significant changes in molecular arrangement.